Modelling effects of social network topology on opinion dynamics during the COVID-19 pandemic

Junxiang Huang[1] and Mikhail Prokopenko[1,2]

[1] Centre for Complex Systems, The University of Sydney, NSW, Australia
[2] Sydney Infectious Diseases Institute, The University of Sydney, NSW, Australia
jhua4833@uni.sydney.edu.au

Abstract. Recurrent waves of infection are influenced by a combination of factors, including seasonal effects, the emergence of new pathogen strains, and fluctuations in human behaviour. Social networks play a key role in shaping individual perceptions of infection risk. However, capturing the complex influence of social media on individual attitudes toward public health measures — such as social distancing — remains a significant modelling challenge. In this study, we investigate how social network topology impacts opinion dynamics related to risk during a pandemic. Building on a previously calibrated and validated agent-based model of the COVID-19 pandemic, we incorporated a social network layer to simulate the spread of risk perception. This enabled us to compare the effects of different network structures on the emergence of recurrent waves. Our simulations indicate that networks exhibiting both scale-free and small-world properties most closely reproduce real-world infection dynamics.

Keywords: Opinion Dynamics, Network Analysis, Agent-based Model

1 Introduction

Recurrent waves of infection have been observed during many pandemics [24, 3]. The factors causing these dynamics include seasonal effects, emergence of new pathogen strains, and varying human behaviour [15, 8]. The recent COVID-19 pandemic has also been characterised by recurrent waves of incidence. The recurrent pattern has become particularly prominent once highly transmissible variants of concern, such as the Omicron variant of SARS-CoV-2, began to dominate the circulation [7]. Several studies have attempted to explain the emergence of recurrent COVID-19 waves, attributing this phenomenon to varying levels of partial lockdowns based on non-pharmaceutical interventions (e.g., social distancing) [7], diminishing vaccine efficacy and re-infections [23], emergence of sub-lineages within the variants of concern [11], and so on.

In tracing the effects of social distancing on the recurrent waves generated by the Omicron variant in Australia, a recent study identified varying opinion dynamics as a significant contributing factor [8]. The agent-based model (ABM) proposed by [8] quantified the probability of individual decisions (e.g., whether or not to adopt social distancing) based on the risk of infection perceived by an

individual. This probability included a combination of self-evaluated risks and the risks perceived via peer pressure, based on opinions of (A) other household members and (B) work/study colleagues. However, the scope of the evaluated peer pressure did not account for diverse interactions within a social network.

In our study, we replace component (B), i.e., interactions with work/study colleagues, by interactions within a social network. This explicitly accounts for risk perceptions influenced by individuals not in direct contact with each other. That is, the infection-transmission interactions and the opinion formation influences are assumed to follow different paths. Using an ABM, extended with opinion dynamics based on influences within a constructed social network, we simulate the COVID-19 incidence characterised by recurrent infection waves.

2 Methods

2.1 Agent-based Modelling and Simulation

To examine effects of opinion dynamics on the pandemic spread, we employed agent-based modelling (ABM). Agent-based models (ABMs) offer a computational framework for simulating person-to-person transmission within a population. These models capture interactions across various settings — such as household, neighbourhoods, communities, workplaces and schools — while also accounting for daily movement between them.

In this study, we extended an ABM implemented in software simulator, "Agent-based Model of Transmission and Control of the COVID-19 pandemic in Australia" (AMTraC-19) [5, 4, 6, 8]. AMTraC-19 has previously been calibrated using the Australian Bureau of Statistics data representing the most recent national census (2021). It comprises 25.4 million anonymous agents with relevant demographic attributes, including age, gender, residential area, and workforce/educational groups. These attributes shape the social environments where interactions between agents — and hence, disease transmission — occur [8].

The ABM captures various aspects relevant to pandemic transmission, including the disease's natural history, pharmaceutical and non-pharmaceutical interventions (NPIs), risk evaluation and opinion dynamics in response to pandemic conditions. The disease transmission parameters, as well as vaccine and immunity parameters, have been previously calibrated and validated [8].

The model is simulated in discrete-time. During transmission, the infection probability for exposed agents depends on both vaccination status and NPIs compliance. Modelled NPIs include Case Isolation (CI), Home Quarantine (HQ), School Closures (SC), and Social Distancing (SD) [5, 8, 18]. The latter comprises a range of transmission-reducing measures beyond mere physical distancing, e.g., mask wearing. Social Distancing allows susceptible agents to reduce their risk of infection. Case Isolation applies to all infected agents, symptomatic or not, who isolate to reduce the likelihood of onward transmission. Home Quarantine is enacted by household members when another member becomes infected; it increases within-household transmission risk while reducing external spread.

School Closure suspends or limits educational activities, (partially) eliminating school-based transmission during the closure period. The fraction of population compliant or adopting Social Distancing can vary over time, being a major variable of our interest, while fractions of populations compliant with other NPIs remain static once activated.

An agent's decision to engage in Social Distancing is influenced by three components: individual disposition, risk self-evaluation, and risk-opinion dynamics. Self-evaluation involves the agent's assessment of perceived infection risk, accounting for perceived infection rate, behavioural fatigue, and observed incidence over a "memory horizon", defined as the agent-specific time window used to assess recent infection trends [8]. Opinion dynamics is modelled through the weighted average of opinions among the agent's social contacts. Agent dispositions include inflexible, flexible and contrarian agents.

2.2 Social Network Modelling

We extended AMTraC-19 with a social network component which simulates influences of social media or a social network in general. In the social network, each node is an AMTraC-19 agent, while edges form connections along which opinions regarding the infection risk can propagate [9, 10]. This emphasises the role of highly connected individuals (influencers) who disproportionately affect the opinion dynamics. The integration of social network component within a pandemic ABM allowed us to explore how the network topology influences the opinion formation and dynamics, ultimately affecting the pandemic incidence.

We computed several network characteristics: clustering coefficient [22, 17, 1], average path length [21, 1], small-world coefficient σ [14], small-world measure ω [19], and degree distribution. Given the very large size of network (around 15 million nodes), some of these characteristics could not be computed within reasonable time, and were estimated by random sampling of thousands of nodes and averaging their local values.

In this study we will examine effects of three social networks topologies. The first social network, labelled SN1, combines a simple lattice configuration model inspired by random graph null models [12] and Watts-Strogatz model [22]. The network implementing our lattice configuration model is labelled SN2. The network constructed following Watts-Strogatz model [22] is labelled SN3. For consistency of our comparative analysis, all networks have exactly the same number of nodes and similar degrees.

Network construction using the canonical Barabasi-Albert model [2] is time consuming for large-scale population (e.g., national level). Hence, we initialised SN1 and SN2 using a simple lattice configuration model [12]. Specifically, the process begins by generating a degree sequence that follows a power-law distribution. Each agent is then connected to its k nearest neighbours, where k equals the degree assigned to that agent. If a connection between two agents already exists, it is considered connected and no additional edge is added. This completes construction of SN2. For SN1, there is an additional step which involves random

rewiring, using rewiring probability of 0.1, as described in the Watts-Strogatz model [22], to enhance clustering and generate small-world properties.

2.3 Opinion Dynamics Modelling

Agent Characteristics. The population was divided into four groups: Inflexible Compliant, Inflexible non-Compliant, Flexible and Contrarian. Flexible and Contrarian agents either choose to "live as usual" or comply to social distancing. The behaviour for these two agent types balances self-evaluation and opinion dynamics. Contrarian agents always choose the opposite decision, relative to the decision of a flexible agent. There simulation included 25% of population as Inflexible Compliant, 25% as Inflexible Non-compliant agents, 10% as Contrarian agents (which is 20% of non-inflexible population), and the rest of population as Flexible agents. Our approach follows [8] in defining several key variables.

Self-evaluation. The perceived risk of infection of a flexible agent i is defined as follows

$$E_i^S(d,T) = 1 - (1-\beta)^{\bar{I}(d,T)} \tag{1}$$

where d is the specific day of simulation, $\beta \in [0,1]$ is the probability of infection that quantifies the agent's risk perception, and T is the time horizon (3).

The normalised moving average of daily incidence is another key variable:

$$\bar{I}(d,T) = \frac{N^c}{N^n}\frac{1}{T}\sum_{r=0}^{T-1} I(d-1-r) \tag{2}$$

where $\frac{N^c}{N^n}$ is the ratio between sizes of a typical community and the overall population of Australia: $N^c = 1000$ and $N^n = 25.4 \times 10^6$ respectively, and $I(d)$ represents incidence at day d.

The agent time horizon $T(d)$ represents the period over which each agent evaluates the infection risk:

$$T(d) = \frac{u}{1+e^{-v(d-L)}} + T(0) \tag{3}$$

with the parametrisation following [8]: $u = 28$, $v = 0.25$, $L = 60$ and $T(0) = 7$.

The pandemic fatigue captures the individual tendency of becoming less motivated to adopt social distancing as time progresses as follows:

$$\beta(d) = \beta_0(1-\gamma)^d \tag{4}$$

where γ is the perception fatigue rate with value of 0.0002, and $\beta_0 = 0.0001$ [8].

Social Influence. The set of social network neighbors of agent i is denoted $N(i)$. The opinion weight of agent $j \in N(i)$, relative to agent i, is denoted $W_j^{SN}(i)$ and is set to be proportional to the degree of agent j:

$$W_j^{SN}(i) = \frac{k_j}{\sum_{x \in N(i)} k_x} \tag{5}$$

The opinion dynamics is generated by two separate sources, households and social media. The corresponding contributions, denoted φ, represent the weights of specific opinion dynamics sources: φ_{HH} for households, and φ_{SN} for social media influences. In this study, we set $\varphi_{SN} = \varphi_{HH} = 0.5$. Denoting the set of agents within a household as A_{HH}, we define the infection risk perceived through social influences as follows:

$$E_i^p(d,T) = \varphi_{SN} \sum_{j \in N(i)} W_j^{SN}(i) E_j^s(d,T) + \varphi_{HH} \frac{1}{|A_{HH}| - 1} \sum_{j \in A_{HH} \setminus \{i\}} E_j^s(d,T) \tag{6}$$

for households with two persons or more, $|A_{HH}| > 1$. For single-person households, only the first term remains.

The overall infection risk combines the risks produced by social influences and self-evaluation:

$$E_i(d) = \lambda E_i^P(d) + (1 - \lambda) E_i^S(d) \tag{7}$$

where the weight of social influences is specified as $\lambda = 0.4$, and the weight of self-evaluation is $1 - \lambda$.

3 Results

3.1 Comparison across constructed networks

In this subsection, we compare the constructed social networks in terms of their topological characteristics. For example, Figure 1 shows that the degree distribution of SN1 follows a power law sufficiently well, with the power law exponent of about 2.35 and the average degree of 23.38.

Average Path Length. As shown in Table 1, both SN1 and SN3 have a considerably shorter average path length, whereas SN2 has a longer average path length due to its lattice-like structure. All networks have a significantly shorter path length than their equivalent lattice networks. Networks SN1 and SN3 have path lengths comparable to those of equivalent random networks, with the path length of SN1 being slightly shorter. Although SN1 is not directly constructed using the Barabási–Albert model, it shares similar properties. Notably, Barabási–Albert networks are known to exhibit lower average path lengths than the equivalent random networks of any size [1], which aligns with the observed behavior of SN1.

Clustering Coefficient. As shown in Table 1, all three networks have a higher clustering coefficient than the clustering coefficient of an equivalent random network. Notably, that the clustering coefficient of SN2, a lattice-like network with a power-law degree distribution, is higher than the estimated clustering coefficient of an equivalent lattice network. Such cases are rare but have been reported for other networks, e.g., “Film actors” network [22].

Small-World coefficient σ. This coefficient is known to be influenced by the network size [16], therefore, its absolute value may not be informative. Table 1 shows that both SN1 and SN3 have a much higher value of σ than SN2, indicating that SN1 and SN3 are closer to small-world networks. When comparing SN1 to SN3, we note that SN1 have a higher value of σ than SN3 (approximately two times higher). This is explained by a higher clustering coefficient and a lower average path length of SN1.

Small-World measure ω. A network is considered to be closer to a lattice network if ω is more negative. In contrast, a network is considered to resemble a random network when ω is more positive. Finally, the small world topology is expected when ω is near zero [16]. Table 1 shows that, using this measure, SN3 is almost perfectly a small-world network: this is not surprising because it is constructed using Watts-Strogatz model [22]. Moreover, SN2 produced $\omega = -1.18$, which falls outside of the expected interval [19], i.e., outside of $[-1, 1]$. A possible reason for this anomaly is that this is a lattice-like network without any random connections, yet with a power-law degree distribution (i.e., having super hubs). Network SN1 has a moderate value of $\omega = 0.36$, and this proximity to zero indicates that this hybrid social network exhibits some small-world properties.

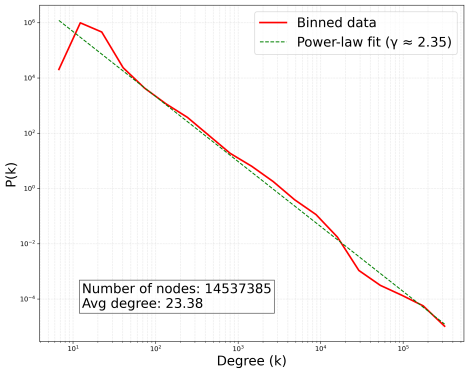

Fig. 1. Degree distribution of social network SN1, shown on a log-log scale using binned rater than discrete degrees. The power-law fit yields the exponent $\gamma \approx 2.35$.

3.2 Pandemic Simulation

As shown in Figure 2, the baseline simulation provides a reasonable fit to the real incidence data, particularly for the first peak, but somewhat diverges for subsequent waves. The ABMs extended with a social network component, based on a constructed social network (SN1, SN2 or SN3) also yield a reasonable match to observed incidence. However, SN1 outperforms the other two networks, as

Table 1. Comparison of social networks in terns of their topological characteristics. SF: Scale-free topology, and SW: Small-world topology. Clustering coefficient and average path length are estimated by sampling 100,000 and 1,000 nodes respectively.

Social Network	Average Degree	Clustering Coefficient	Average Path Length	Topology	Small-World coefficient σ	Small-World measure ω
SN1	23.38	0.62	4.29	SF+SW	469751	0.36
SN2	23.35	0.85	4381.98	SF	629.21	-1.18
SN3	24	0.53	7.46	SW	223832	-0.04
Random	23.38	1.6084×10^{-6}	5.23	Random	1.00	1.00
Lattice	23.38	0.72	310868	Lattice	7.53	-1.00

evidenced by a good fit to the actual incidence curve. Networks SN2 and SN3 produce similar incidence curves before the second peak, however, the incidence peaks generated by SN2 are lower than those of SN3 during both the second and third waves. Importantly, the simulations based on social networks with super-hubs (scale-free properties) tend to produce more volatile dynamics, as reflected in the comparatively larger standard deviation.

Table 2. Comparison of simulation results with respect to real incidence data using different social networks. MAPE represents Mean Absolute Percentage Error. The null hypothesis is that the baseline and alternative approaches have the same forecast accuracy. It is evaluated using Diebold-Mariano test [13].

Social Network	MAPE	MAPE (day 25 to 150)	p-value	null hypothesis
SN1	40.73%	25.17%	0.0485	rejected
SN2	41.60%	26.74%	0.0492	rejected
SN3	42.46%	26.50%	0.882	accepted
Baseline	41.10%	27.10%	N/A	N/A

Table 2 summarises a comparison of simulation results produced by the ABM extended with SN1, SN2 or SN3. We observe that SN1 — a network combining scale-free and small-world properties —outperforms the alternatives. The SN2 alternative constructed to match a scale-free network produces the incidence profiles which are similar to the baseline. Finally, SN3 — a predominantly small-world network — underperforms relative to the baseline. The comparison is based on the Mean Absolute Percentage Error which measures the mean distance between the simulated and actual incidence profiles. Importantly, Diebold-Mariano test [13] establishes that only SN1 and SN2 alternatives have different predictive accuracy compared to the baseline.

However, if the time period used for comparison is limited to the interval between days 25 and 150, that is, the period covering formation of the first and second waves which preceded the emergence of a new sub-lineage (Omicron BA.2), we observe a slightly different result. For this period, the three network-based

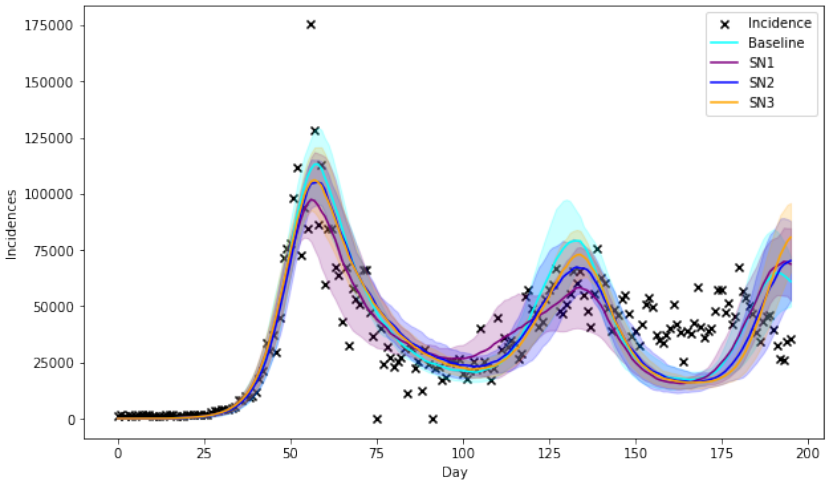

Fig. 2. The incidence profiles obtained by ABM simulation using each of the three social networks, as well as the baseline ABM without a network component [8]. Other parameters are kept constant. The averaged incidence is shown as solid curves, while the shaded areas represent the range of standard deviation obtained over 12 runs. Actual incidence data are shown with crosses.

models outperformed the baseline. Networks SN2 and SN3 generated similar results, while SN1 again outperformed the alternatives.

4 Discussion and Conclusion

Recurrent waves of infection can be partially attributed to the way individuals perceive and respond to risk, which can shift rapidly in response to both personal experiences and social influences. Social networks — both offline and online — play a critical role in shaping these perceptions. We aimed to understand the relationship between social network structure and the dynamics of risk perception during a pandemic. To do so, we extended an existing agent-based model (AMTraC-19) that had previously been calibrated and validated using real-world data from the COVID-19 pandemic. We augmented this framework by integrating a social network layer, allowing agents to influence one another's perception of infection risk based on their connections within the network.

Our simulation results demonstrated that ABM extended with the opinion network which exhibits both scale-free and small-world characteristics is more effective in reproducing the recurrent wave patterns observed in real-world pandemic data (e.g., reported in Australia during 2022). These findings suggest that the structure of social networks plays an important role not only in shaping individual risk perception but also in influencing broader epidemic dynamics. This work highlights the importance of incorporating realistic social interaction

patterns into epidemiological models, particularly when assessing the potential impact of public health interventions that rely on behaviour change [20].

There are several limitations of this study. First, certain topological properties of the social networks — such as average path length and clustering coefficient — were estimated through sub-sampling, which may introduce some degree of approximation or bias. Another key limitation lies in the assumption that the dominant viral variant remains unchanged throughout the simulation period. Incorporating phylodynamic components into the model could help capture these evolutionary changes and improve alignment with real-world data. Additionally, future work could explore a broader range of social network configurations by applying alternative connection rewiring techniques, thereby allowing for more diverse and realistic representations of social interaction patterns.

Acknowledgement. This work was supported by the Australian Research Council grant DP220101688 (MP). The authors express their thanks to developers of AMTraC-19, especially Sheryl L. Chang, Quang Dang Nguyen, Oliver C. Cliff, Cameron Zachreson and Nathan Harding, as well as members of the project team: Carl J. E. Suster, Rebecca J. Rocket, Christina M. Jamerlan, Alexandra Martiniuk, Vitali Sintchenko and Tania C. Sorrell. The authors also acknowledge the Sydney Informatics Hub and the use of the University of Sydney's high performance computing cluster, Artemis. The source code of AMTraC-19 is available at Zenodo [6].

Declaration of Interest The authors have no competing interests.

References

1. Albert, R., Barabási, A.L.: Statistical mechanics of complex networks. Reviews of Modern Physics 74(1), 47–97 (Jan 2002)
2. Barabasi, A.L., Albert, R.: Emergence of scaling in random networks. Science 286(5439), 509–512 (Oct 1999)
3. Campi, G., Bianconi, A.: Periodic recurrent waves of COVID-19 epidemics and vaccination campaign. Chaos, Solitons & Fractals 160, 112216 (2022)
4. Chang, S.L., Cliff, O.M., Zachreson, C., Prokopenko, M.: Simulating transmission scenarios of the Delta variant of SARS-COV-2 in Australia. Frontiers in Public Health 10 (Feb 2022)
5. Chang, S.L., Harding, N., Zachreson, C., Cliff, O.M., Prokopenko, M.: Modelling transmission and control of the COVID-19 pandemic in Australia. Nature Communications 11(1) (Nov 2020)
6. Chang, S.L., Nguyen, Q.D., Zachreson, C., Cliff, O.M., Prokopenko, M.: AMTraC-19 source code: Agent-based model of transmission and control of the COVID-19 pandemic in Australia (Apr 2024)
7. Chang, S.L., Nguyen, Q.D., Martiniuk, A., Sintchenko, V., Sorrell, T.C., Prokopenko, M.: Persistence of the Omicron variant of SARS-COV-2 in Australia: The impact of fluctuating social distancing. PLOS Global Public Health 3(4) (Apr 2023)

8. Chang, S.L., Nguyen, Q.D., Suster, C.J.E., Jamerlan, C.M., Rockett, R.J., Sintchenko, V., Sorrell, T.C., Martiniuk, A., Prokopenko, M.: Impact of opinion dynamics on recurrent pandemic waves: Balancing risk aversion and peer pressure. Royal Society Interface Focus, accepted (2025)
9. Chang, S.L., Piraveenan, M., Prokopenko, M.: Impact of network assortativity on epidemic and vaccination behaviour. Chaos, Solitons & Fractals 140, 110143 (2020)
10. Chang, S.L., Piraveenan, M., Prokopenko, M.: The effects of imitation dynamics on vaccination behaviours in SIR-Network model. International Journal of Environmental Research and Public Health 16(14) (2019)
11. Chatterjee, S., Bhattacharya, M., Nag, S., Dhama, K., Chakraborty, C.: A detailed overview of SARS-CoV-2 Omicron: Its sub-variants, mutations and pathophysiology, clinical characteristics, immunological landscape, immune escape, and therapies. Viruses 15(1), 167 (Jan 2023)
12. Fosdick, B.K., Larremore, D.B., Nishimura, J., Ugander, J.: Configuring random graph models with fixed degree sequences. SIAM Review 60(2), 315–355 (Jan 2018)
13. Harvey, D., Leybourne, S., Newbold, P.: Testing the equality of prediction mean squared errors. International Journal of Forecasting 13(2), 281–291 (1997)
14. Humphries, M., Gurney, K., Prescott, T.: The brainstem reticular formation is a small-world, not scale-free, network. Proceedings of the Royal Society B: Biological Sciences 273(1585), 503–511 (Nov 2005)
15. Milne, G.J., Carrivick, J., Whyatt, D.: Mitigating the SARS-COV-2 Delta disease burden in Australia by non-pharmaceutical interventions and vaccinating children: A modelling analysis. BMC Medicine 20(1) (Feb 2022)
16. Neal, Z.P.: How small is it? Comparing indices of small worldliness. Network Science 5(1), 30–44 (2017)
17. Newman, M.E.: Models of the small world. Journal of Statistical Physics 101(3/4), 819–841 (Nov 2000)
18. Nguyen, Q.D., Chang, S.L., Jamerlan, C.M., Prokopenko, M.: Measuring unequal distribution of pandemic severity across census years, variants of concern and interventions. Population Health Metrics 21(1) (Oct 2023)
19. Telesford, Q.K., Joyce, K.E., Hayasaka, S., Burdette, J.H., Laurienti, P.J.: The ubiquity of small-world networks. Brain Connectivity 1(5), 367–375 (Dec 2011)
20. Thompson, J., McClure, R., Scott, N., Hellard, M., Abeysuriya, R., Vidanaarachchi, R., Thwaites, J., Lazarus, J.V., Lavis, J., Michie, S., et al.: A framework for considering the utility of models when facing tough decisions in public health: A guideline for policy-makers. Health Research Policy and Systems 20(1) (Oct 2022)
21. Watts, D.J.: 2. An Overview of the Small-World Phenomenon, pp. 11–40. Princeton University Press, Princeton (1999)
22. Watts, D.J., Strogatz, S.H.: Collective dynamics of 'small-world' networks. Nature 393(6684), 440–442 (Jun 1998)
23. Wei, J., Stoesser, N., Matthews, P.C., Khera, T., Gethings, O., Diamond, I., Studley, R., Taylor, N., Peto, T.E., Walker, A.S., et al.: Risk of SARS-COV-2 reinfection during multiple Omicron variant waves in the UK general population. Nature Communications 15(1) (Feb 2024)
24. Zhang, S.X., Arroyo Marioli, F., Gao, R., Wang, S.: A second wave? what do people mean by COVID waves? – a working definition of epidemic waves. Risk Management and Healthcare Policy 14, 3775–3782 (Sep 2021)